Atmos. Meas. Tech. Discuss., 7, 12449–12480, 2014
www.atmos-meas-tech-discuss.net/7/12449/2014/
doi:10.5194/amtd-7-12449-2014

Atmospheric Measurement Techniques Discussions

Organic aerosol composition measurements with advanced offline and in-situ techniques during the CalNex campaign

J. Timkovsky[1], A. W. H. Chan[2,*], T. Dorst[1], A. H. Goldstein[2,3], B. Oyama[1,4], and R. Holzinger[1]

[1]Institute for Marine and Atmospheric Research Utrecht, Utrecht University, P.O. Box 80005, 3508 TA, the Netherlands
[2]Department of Environmental Science, Policy, and Management, University of California, Berkeley, California, USA
[3]Department of Civil and Environmental Engineering, University of California, Berkeley, California, USA
[4]Department of Meteorology, Institute of Astronomy, Geophysics, and Atmospheric Sciences, University of São Paulo, Brazil
[*]now at: Department of Chemical Engineering and Applied Chemistry, University of Toronto, Toronto, Ontario, Canada

Received: 7 October 2014 – Accepted: 18 November 2014 – Published: 12 December 2014

Correspondence to: J. Timkovsky (j.timkovsky@uu.nl)

Published by Copernicus Publications on behalf of the European Geosciences Union.

AMTD
7, 12449–12480, 2014

Abstract

Our understanding of formation processes, physical properties and climate/health effects of organic aerosols is still limited in part due to limited knowledge of organic aerosol composition. We present speciated measurements of organic aerosol composition by two methods: in-situ thermal-desorption proton-transfer-reaction mass spectrometry (TD-PTR-MS) and offline two-dimensional gas chromatography with a time-of-flight mass spectrometer (GC×GC/TOF-MS). 153 compounds were identified using the GC×GC/TOF-MS, 123 of which were matched with 64 ions observed by the TD-PTR-MS. A reasonable overall correlation of 0.67 (r^2) was found between the total matched TD-PTR-MS signal (sum of 64 ions) and the total matched GC×GC/TOF-MS signal (sum of 123 compounds). A reasonable quantitative agreement between the two methods was observed for most individual compounds with concentrations which were detected at levels above 2 ng m^{-3} using the GC×GC/TOF-MS. The analysis of monocarboxylic acids standards with TD-PTR-MS showed that alkanoic acids with molecular masses below 290 amu are detected well (recovery fractions above 60 %). However, the concentrations of these acids were consistently higher on quartz filters (quantified offline by GC×GC/TOF-MS) than those suggested by in-situ TD-PTR-MS measurements, which is consistent with the semivolatile nature of the acids and corresponding positive filter sampling artifacts.

1 Introduction

Aerosol particles are ubiquitous in the atmosphere, and are important for two main reasons. Firstly, they scatter and absorb solar radiation, and change cloud properties affecting climate on Earth (Boucher et al., 2013). Secondly, they penetrate into human lungs, causing increased mortality (e.g., Pope and Dockery, 2006). Atmospheric aerosol has various sources, both natural and anthropogenic (e.g., de Gouw and Jimenez, 2009). Organic aerosol (OA) comprises 20 to 90 % of the total aerosol mass

AMTD
7, 12449–12480, 2014

(Kanakidou et al., 2005). OA can be emitted directly (primary OA, POA), but can also be produced in the atmosphere via photochemical oxidation of volatile organic compounds (secondary OA, SOA).

Elucidating aerosol chemical composition is key to understanding sources and formation processes, and to effectively controlling aerosol amounts in the atmosphere (e.g., Ulbrich et al., 2009). For example, n-carboxylic acids are one of the three major classes of organic molecular markers used extensively for OA source apportionment (Sinabut et al., 2005). They are known to be primarily emitted (Legrand and De Angelis, 1996) and produced from secondary photochemical reactions (Kawamura and Sakaguchi, 1999).

During the Calnex campaign Veres et al. (2011) observed a strong correlation of gas phase organic acids concentrations with the oxidants (O_3 and NO_2) concentrations. Vogel et al. (2013) reported that the contribution of organic acids to the total submicron OA can be up to 60 %.

Even though many in-situ techniques have been deployed to study OA composition (e.g., Jayne et al., 2000; Holzinger et al., 2010a; Weber et al., 2001), it is still commonly characterized on the bulk level using descriptors such as oxygen-to-carbon (O/C) ratio, volatility distribution, or total organic carbon mass. Only a limited number of in-situ studies have researched OA at a molecular level using high time resolution (two hourly or better) measurements (e.g., Williams et al., 2014; Yatavelli et al., 2014; Zhao et al., 2013). Therefore, more detailed studies from various locations and time periods are needed to better understand chemical composition and sources of OA.

Here we deployed two different techniques allowing for detailed chemical composition measurements of OA: (1) in-situ thermal-desorption proton-transfer-reaction mass spectrometry (TD-PTR-MS), and (2) offline filter analysis by comprehensive two-dimensional gas chromatography coupled to time-of-flight mass spectrometry (GC×GC/TOF-MS). The in-situ TD-PTR-MS technique was developed at Utrecht University, the Netherlands (Holzinger et al., 2010a, 2013). Organic aerosols are collected and thermally desorbed in-situ, and organic compounds are ionized by proton trans-

AMTD
7, 12449–12480, 2014

fer reaction. As a result, one can identify chemical composition of hundreds of compounds constituting the original aerosol and/or fragments of these compounds. 25–60 % of the total OA has been directly measured with this technique (Holzinger et al., 2013). GC×GC/TOF-MS has been applied to organic aerosol analysis to provide additional separation using two-dimensional gas chromatography (e.g., Hamilton et al., 2004; Kallio et al., 2006). Analysis of the samples described in this work has previously been reported with regard to distinguishing the alkane isomers in unresolved complex mixtures (Chan et al., 2013). Here we focus on compounds with a broader range of functional groups that are clearly resolved using GC×GC/TOF-MS.

In this study we aim to use the GC×GC/TOF-MS measurements of individual compounds and aerosol mass spectrometer measurements of total organic aerosol to better understand the strengths and weaknesses of the TD-PTR-MS technique for measuring individual chemicals and total organic aerosol, respectively. This comparison allows us to provide a broad overview of the aerosol composition using these two complementary techniques. The comparison is done based on two days of measurements during the CalNex (California Research at the Nexus of Air Quality and Climate Change) 2010 campaign in Pasadena, California.

2 Experimental methods

2.1 Measurement campaign

The data presented in this paper were obtained during the CalNex field campaign in Pasadena, California performed from 15 May till 16 June 2010. The site is located approximately 18 km northeast of downtown of Los Angeles on the campus of California Institute of Technology (34.1408° N, 118.1223° W). More than 40 groups participated in this campaign collecting data characterizing chemical composition, transformation and quantity of gas and particle constituents of the atmosphere. The in-situ TD-PTR-MS and aerosol mass spectrometer (AMS) instruments were located in neighboring

AMTD
7, 12449–12480, 2014

air-conditioned containers, and the high volume $PM_{2.5}$ filter sampler was located on the roof of one of the buildings on the campus ~ 200 m southeast of the containers. The inlet for the TD-PTR-MS instrument was located at the top of a 10 m scaffolding tower and was equipped with $PM_{2.5}$ cyclones. The AMS inlet was located 2 m above the roof of the container housing the instrument and AMS instrument measured submicron aerosols (PM_1). Filter samples were collected on quartz fiber filters (TissuquartzTM Filters, 2500 QAT-UP, Pall Life Sciences), which were 20 cm × 25 cm, allowing for high-volume $PM_{2.5}$ sampling at ~ 1 m^3 min^{-1}.

2.2 Instrument description

2.2.1 The in-situ TD-PTR-MS method

In-situ aerosol measurements were carried out with an aerosol sampling unit with two identical inlet systems attached to a proton-transfer-reaction time-of-flight mass spectrometer (PTR-TOF-MS, further referred to as "PTR-MS") (Fig. 1a). The setup has been described in detail elsewhere (Holzinger et al., 2010a, 2013). In short, the air flow passes through 12 m long copper inlet tubes (ID = 6.5 mm), particles are humidified in a humidifier and then they are collected in a collection-thermal-desorption (CTD) cell. Afterwards, the cell is heated up in steps of 50 °C up to 350 °C and the emitted species are carried with a flow of nitrogen (ultrapure nitrogen, 5.7 purity, Air Products) into the PTR-MS. The PTR-MS was operated with the following settings: drift tube temperature, 120 °C, inlet tube temperature, 180 °C; ion source voltages, U_s = 140 V, U_{so} = 92 V; E/N, 130 Td; extraction voltage at the end of the drift tube, U_{dx} = 24 V. The intensity of the primary H_3O^+ ion signal (detected at m/z 21.023) was typically higher than 5×10^5 counts per second (cps).

After the measurements from the first inlet are finished, the valve system is switched automatically to allow aerosol measurements from the second inlet to start. Subsequent to the measurements from the second inlet, gas phase measurements (not con-

AMTD
7, 12449–12480, 2014

sidered in the current paper) are carried out and then the measurement cycle starts over (see Fig. 1 in Holzinger et al., 2013).

2.2.2 Filter sampling with offline GC×GC/TOF-MS analysis

Filter samples were analyzed offline using comprehensive two-dimensional gas chromatography coupled to a time-of-flight mass spectrometer (GC×GC/TOF-MS, hereafter referred to as GC×GC). Details of the analysis method are described in Chan et al. (2013). In brief, filter punches (total area of 1.6 cm^2) were thermally desorbed at 320 °C under helium (TDS3, Gerstel) to a two-dimensional gas chromatograph (Agilent 7890). Comprehensive GC×GC was performed using the Zoex thermal modulator interface, combining a 60 m × 0.25 mm × 0.25 µm non-polar capillary column (Rxi-5Sil MS, Restek) for the first-dimension separation (by volatility) with a medium-polarity second dimension column (1 m × 0.25 mm × 0.25 µm, Rtx-200MS, Restek). The second dimension column was maintained at 15 °C above the main oven temperature using a secondary oven. Effluent from the second column was analyzed using a high-resolution ($m/\Delta m \sim 4000$) time-of-flight mass spectrometer (HR-TOF, Tofwerk, Thun, Switzerland) using 70 eV electron impact ionization. Peak detection and compound identification was performed using GC Image software (LLC). Around 1100 peaks were measured at above detection limits. Compounds were identified by confirmation with authentic standards or by mass spectral library search, or, in some cases, based on a unique ion (such as m/z 85 for gamma lactones, 217 for steranes) and its location in the 2-dimensional chromatogram. Identification of otherwise unresolved branched and cyclic alkanes has also been done on these samples using soft ionization with vacuum ultraviolet radiation (Chan et al., 2013) but these alkanes are not included among the compounds discussed here.

Among the 1100 resolved peaks, the 153 compounds reported here were positively identified with the GC×GC technique, classified by compound groups: aromatic esters, benzofuranones, oxygenated polycyclic aromatic hydrocarbons (oxyPAHs), phthalates, 2-alkanones, 3-alkanones, alkanoic acids, alkyl esters, delta-lactones, gamma-

AMTD
7, 12449–12480, 2014

lactones, nitrogen-containing aromatic compounds (N-aromatic), polycyclic aromatic hydrocarbons (PAHs), sulfur-containing compounds (S-compounds), amides, hopanes, alkanes and several compounds were identified at a single m/z value (multiple). Another 31 compounds were classified into these compound groups without positive identification. Compound class nicknames are presented in the brackets and further used in the article to refer to them.

2.2.3 Aerosol Mass Spectrometer (AMS)

The AMS measurements used in the current study has been described previously in detail (Hayes et al., 2013). In short, AMS allows for measurements of nonrefractory submicron aerosol (organic and inorganic) (DeCarlo et al., 2006). The operational principle of AMS can be presented briefly as follows. Air is sampled through a critical orifice with a consecutive focusing, acceleration and separation of particles by size. Next, particles are vaporized at 600 °C, ionized by electron ionization (70 eV) and detected with a high resolution time-of-flight mass spectrometer. Details of AMS operation and data analysis can be found in Hayes et al. (2013).

2.2.4 Preparation and measurement of standards

In this paper we present measurements of two types of standards: single compounds and a mixture of compounds. The following single compounds were measured: decanoic, pentadecanoic and octadecanoic acids. Known quantities of each acid were first dissolved in ethanol, and then an aliquot of the solution containing 10 µg of a substance was placed on a quartz filter with a diameter of 5 mm. Next, two minutes were allowed to let most of the solvent evaporate before the filter was inserted in the oven, which is a part of the offline TD-PTR-MS system described in detail by Timkovsky et al. (2015) (Fig. 1b). Each measurement was repeated 3 times, and 2 blank filters were measured at the beginning and at the end of each measurement sequence.

AMTD
7, 12449–12480, 2014

A mixture containing 77 representative organic compounds and C8–C40 alkanes (this mixture is further called "multicomponent mixture") was carefully prepared by dissolving respective compounds in deuterated acetone. An aliquot of the solution with 0.062 to 20 ng of the substances was placed on quartz filters. In this paper we focus only on acids contained in this standard (21 acids). Again, three filter replicas and two blank filters were measured with the offline TD-PTR-MS.

The filter measuring procedure is described in detail by Timkovsky et al. (2015). In short, the sample is placed in the oven and allowed to stabilize for two minutes. Next, the temperature of the oven is increased stepwise from 100 to 350 °C in increments of 50 °C every 3 min. The desorbed compounds are carried by the 200 mL min^{-1} flow of nitrogen (ultrapure nitrogen, 5.7 purity, Air Products) into the PTR-MS. The operating conditions of the PTR-MS were the same as for the in-situ TD-PTR-MS measurements (see Sect. 2.2.1).

2.3 Data treatment

2.3.1 In-situ and offline TD-PTR-MS data

Data evaluation was done with Interactive Data Language (IDL, version 8.1.0, ITT Visual Information Solutions) using custom made routines described by Holzinger et al. (2010b). The initial mass lists consisted of 717 and 748 masses for multicomponent mixture and CalNex measurements, respectively. Ions associated with primary ions and contaminations from the ion source were removed from the mass lists by filtering out $m/z < 40$ amu (except for m/z 31.017 and 33.033). Inorganic ions (i.e. ions in the m/z range 40–50 Da, that were matched with an inorganic formula) were also removed from the mass lists. Finally, the mass lists contained 653 and 726 masses for standard and CalNex measurements, respectively. The mixing ratios of ions were calculated from the measured intensities by applying the same protonation reaction rate constant for all ions (3×10^{-9} cm^3 s^{-1} molecule^{-1}) (Holzinger et al., 2010b).

AMTD
7, 12449–12480, 2014

For the in-situ data analysis, the initial mass spectra were first averaged to obtain data with a time resolution of 5 s. Second, the data were averaged over the measured temperature step (3 min each) and the data for all temperature steps were summed. Third, the resulted mixing ratios were converted to mass concentrations for individual ions by multiplying by ion molecular mass, volume of nitrogen used for desorption for one measurement cycle and dividing by the volume of air sample from which aerosols were collected. Forth, the data from inlet A and B were merged and averaged to match the filter sampling times. Fifth, the resulted mass concentrations were averaged over the whole comparison period (30–31 May) for the data presented in Sect. 3.2.2. The maximum total uncertainty of ~ 54 % (mostly due to the uncertainty of the reaction rate coefficient) was calculated for these mass concentration based on the method described by Timkovsky et al. (2015).

The same two initial steps were taken for the analysis of the offline TD-PTR-MS data. The obtained data with a 3 min resolution were processed according to the procedure described in Timkovsky et al. (2015). In short, the instrument background and blank corrected mass at a single temperature step (A_T) was calculated according to Eq. (1):

$$A_T = (\mathrm{VMR}_{i,0} - \mathrm{VMR}_{i,\mathrm{instrbgd}} - (\mathrm{VMR}_{i,\mathrm{fb}} - \mathrm{VMR}_{i,\mathrm{instrbgd_{fb}}})) \cdot M_i \cdot V_{\mathrm{nitrogen}} \quad (1)$$

where $\mathrm{VMR}_{i,0}$ is the uncorrected mixing ratio of the ion i, and $\mathrm{VMR}_{i,\mathrm{fb}}$ is the mixing ratio of the ion i observed on the field blank, $\mathrm{VMR}_{i,\mathrm{instrbgd}}$ and $\mathrm{VMR}_{i,\mathrm{instrbgd_{fb}}}$ are the instrument background mixing ratios of the ion i observed during the sample and field blank measurements, respectively (all in nmol mol^{-1}). M_i is the molecular weight of the ion i (minus one amu) and V_{nitrogen} is the volume of nitrogen used for desorption at a single temperature step in mol. As a next step, the six masses A_T measured for the 50 °C intervals between 100 and 350 °C were summed to obtain the total mass of the substance which then compared with the known amount of the substance initially placed on the filters.

AMTD
7, 12449–12480, 2014

2.3.2 GC×GC quantification

GC×GC data were analyzed using GC Image (LLC). Peak volumes of quantification ions were used to calculate compound signal, and then converted to the total ion signal based on ratios calculated from mass spectra in the NIST08 library. The total ion signals were then converted to on-column mass based on mass calibrations conducted using a representative set of commercially available organic compounds as external standards. For those compounds not commercially available, surrogate standards were assigned based on similarities in molecular structure. Deuterated internal standards were also used to correct for run-to-run variability in instrument response. Mass concentrations were then calculated based on the ratio of filter punch area to total filter area and sampling flow rate.

2.3.3 Mass matching process

In order to match ions measured by the TD-PTR-MS with compounds put on the filters and those measured with the GC×GC technique (further referred to as "known compounds") the following procedure was applied. First, we assumed that all known compounds were detected at their protonated mass, or in the case of oxygenated compounds at the dehydrated fragment (i.e. protonated mass −18.010, the molecular weight of the H_2O fragment). Other fragmentation patterns are possible, but not considered here. We matched the protonated and fragment masses with the ion masses detected by the TD-PTR-MS. A match was assigned if the difference between the protonated or fragment mass of the known compound and an ion detected with the PTR-MS was smaller than 250 ppm (corresponding to the mass resolution of the PTR-MS). Compounds were considered as not detected when either the detected amount by the TD-PTR-MS was negative after background subtraction or the abovementioned difference was above 250 ppm.

In the case where only one of these ions (parent or fragment) was present in the PTR mass list, the signal of this single ion was attributed to the known compound.

AMTD
7, 12449–12480, 2014

If a M_r obtained after 18.010 amu subtraction was equal to the M_r already present in the mass list with matches, the intensities of these two masses were summed and the corresponding ions were further considered as isobars. The concentrations of the compounds measured with the GC×GC technique and corresponding to the two masses were also summed. The mass value of the ion with lowest m/z value in the group, i.e. fragmented ion, was chosen to represent this group of ions. For example, 6H-Indolo[3,2,1-de][1,5]naphthyridin-6-one was detected at m/z 221.089 amu and its fragment was detected at m/z 203.087 Da. However, fluoranthene and pyrene were also detected at 203.087 Da. Consequently, 6H-Indolo[3,2,1-de][1,5]naphthyridin-6-one, fluoranthene and pyrene were considered as a single compound with M_r of 203.087 Da, and their measured concentrations were summed in both TD-PTR-MS and the GC×GC data. Whenever more than one compound was measured at the same mass, the most abundant compound (based on the GC×GC measurements) from the considered group was chosen to represent all of the compounds. For example, phenaleno[1,9-bc]thiophene and anthraquinone were detected at the same m/z value (209.059 Da) with the TD-PTR-MS technique. The total averaged mass concentration of phenaleno[1,9-bc]thiophene and anthraquinone was 1.57 and 27.70 ng m^{-3}, respectively (based on the GC×GC measurements). Thus, anthraquinone represents 95 % of the signal at that mass, and all of the signal at 209.059 amu was attributed to anthraquinone. In the case where structural isomers were identified with the GC×GC technique, the corresponding GC×GC concentrations were summed. Mass concentrations of 22 alkanes measured by the GC×GC were summed and all alkanes were considered as one compound with M_r of 113.133 Da as all alkanes are detected with the PTR-MS at the same set of masses (43.055, 57.070, 71.086 Da, and a few other masses). This resulted in the decrease of the GC×GC dataset, from 153 to 132 compounds.

Applying these rules we were able to match 123 of the 132 distinguishable compounds measured with the GC×GC technique, to corresponding 64 ions measured with the TD-PTR-MS technique (see Table A1). The contribution of the unidentified 9

AMTD
7, 12449–12480, 2014

compounds is minor (< 2 %) compared to the total mass concentration of the 123 compounds. While we applied rather relaxed rules when attributing detected m/z values to known compounds, we found that in practice the matches were much closer than 250 ppm: the median difference for 64 ions was 41 ppm.

3 Results

3.1 Monocarboxylic acid standards measured by the TD-PTR-MS

To calibrate the in-situ TD-PTR-MS technique for measurements of monocarboxylic acids, a series of filters with known quantities of the acids were prepared and measured with the offline setup. Figure 2 shows the ratio of the detected amount of substance and the amount of monocarboxylic acids that was applied on the filter, i.e. fraction of acid recovered. The measurements of single compounds (pink triangles in Fig. 2) and the multicomponent mixture (blue triangles and black crosses in Fig. 2) are shown together in this figure. Only the signal of the protonated ion has been used to calculate mass concentrations of alkanoic acids measured with the offline TD-PTR-MS technique. In total, 24 monocarboxylic acids are measured (Fig. 2). The lowest fractions (i.e. lower amounts detected by the TD-PTR-MS) are observed for the high molecular mass acids (M_r > 300 Da). This could be caused by significantly lower than 100 % desorption efficiency off the filters at temperatures up to 350 °C and thermal decomposition of these high molecular weight substances (e.g., charring) (Yu et al., 2002).

Five out of the 21 monocarboxylic acids (M_r > 305 Da) that were put on the filters in the multicomponent mixture were not detected with the offline TD-PTR-MS technique (bold in Table 1). This might be caused by the fact that these acids (except for triacontanoic acid) have the highest background signal among the acids with M_r > 305 Da. Triacontanoic acid is the heaviest acid injected onto the filters and likely indicates the lower volatility limit of the compounds which could be measured with the offline TD-PTR-MS technique. Other heavy monocarboxylic acids (M_r > 300 Da) are strongly un-

AMTD
7, 12449–12480, 2014

derestimated with the offline TD-PTR-MS technique (fraction of acid recovered ≤0.04). Therefore, we can generally conclude that heavy acids (M_r > 300 Da) are not detected well with this technique, which is likely caused by some of the aforementioned reasons.

Alkanoic acids with M_r < 290 amu are detected reasonably well (fractions recovered above 60 %, Fig. 2). Acids containing one or more double bonds with M_r < 290 amu (further referred to as "n-enoic acids") are not detected as well (less than 38 %), which is possibly caused by their higher affinity to quartz filters and lower resistance to thermal decomposition. The higher affinity leads to a release at higher temperatures, so that thermal decomposition becomes a competitive desorption pathway and eventually dominates over evaporation.

Based on the presented measurements, a calibration factor for alkanoic acids with M_r < 290 amu is developed. Using the averaging of the fractions recovered of 6 alkanoic acids with M_r < 290 amu (3 single standards and 3 from the multicomponent mixture), a calibration factor of 1.45 is found, and applied to the alkanoic acid concentrations discussed in Sects. 3.2.2 and 3.2.3. There are three likely explanations for the higher than unity calibration factor. First, the same reaction rate coefficient is applied to mixing ratio calculations of all compounds measured by the PTR-MS, and the real reaction rate coefficient for alkanoic acids can be lower than applied (Zhao and Zhang, 2004). Second, a partial thermal decomposition of the acids may occur on filters. Third, lighter alkanoic acids could have (e.g., decanoic) evaporated off of the filter before the filter was placed in the oven for analysis. The first reason is, however, less likely because similar measurements of 3 alkanoic acids with M_r < 290 amu on aluminum foil indicated that the total amount of the acids can be observed with the offline TD-PTR-MS technique for the heavier acids (penta- and octadecanoic acids), while a lower fraction (more loss through evaporation) is observed for the lighter decanoic acid.

AMTD
7, 12449–12480, 2014

3.2 Comparison of the in-situ TD-PTR-MS and offline GC×GC data

3.2.1 Total measured OA signal

In Fig. 3 we present the time series of total OA mass concentrations measured by the in-situ TD-PTR-MS and the AMS instruments (further named "total OA_PTR" and "total OA_AMS", respectively), the total concentration of the 123 compounds measured by the GC×GC, and the total concentration of the corresponding 64 masses measured by the TD-PTR-MS (further named "123 compounds_GC×GC" and "64 masses_PTR", respectively) over 2 days. The 64 masses constitute 25 % of the total OA mass measured by the TD-PTR-MS.

In general, the total OA_PTR and the total OA_AMS correlate well with a correlation coefficient (r^2) of 0.84. The average percentage of the total OA detected by the TD-PTR-MS is 33 %. Potential reasons for undetected OA by the TD-PTR-MS, that is fragmentation in the PTR-MS and thermal decomposition in the CTD cell, have been discussed in Holzinger et al. (2013).

A reasonable qualitative and quantitative correlation is observed between the 123 compounds_GC×GC and the 64 masses_PTR: a correlation coefficient (r^2) equals to 0.67. On average, the TD-PTR-MS detected 98 % of the total mass of the "123 compounds_GC×GC". However, one can notice that the correlation between the 123 compounds_GC×GC and the 64 masses_PTR is better during the first than the second day of the measurements. This might relate to a different wind direction during the second day and to the fact that the TD-PTR-MS and the HiVol filter sampler were located ~ 200 m apart during the campaign. Indeed, the prevailing wind directions were northeast on 30 May and northwest and west on 31 May, based on 48 h back trajectories using the model HYSPLIT (Draxler and Rolph, 2013; Rolph, 2013).

AMTD
7, 12449–12480, 2014

3.2.2 Comparison by compound class

Figure 4 presents mass concentrations of compounds measured with the in-situ TD-PTR-MS technique vs. corresponding mass concentrations measured with the GC×GC technique (referred to as "PTR" and "GC×GC", respectively) averaged over the whole comparison period with 1 : 1 line shown for reference. Compound classes are shown according to the scheme introduced in Sect. 2.2.2.

In general, the concentrations of organic species measured with the two techniques agree reasonably well for most compounds with mass concentrations above $\sim 2\,\mathrm{ng\,m^{-3}}$ as measured by GC×GC (see the thin black lines above and below the 1 : 1 line in Fig. 4 that mark the $0.25 < \mathrm{PTR} / (\mathrm{GC{\times}GC}) < 2$ boundaries). The PTR / (GC×GC) ratio indicates the ratio of the amount of a substance measured with the TD-PTR-MS technique to the amount of the substance measured on the filters with the GC×GC technique. The ratio is expected to be within the boundaries of 0.5 and 2 if the accuracy for both, TD-PTR-MS and GC×GC, is 33 %. An accuracy of 54 % for TD-PTR-MS and 40 % for GC×GC is consistent with wider boundaries of 0.4 and 3.2. The upper boundary (2) suggested by Fig. 4 is lower than the upper boundary suggested by the stated accuracy levels (3.2). This may indicate that the stated accuracy levels are an overestimate of the real accuracy. The lower boundary (0.25) suggested by Fig. 4 is somewhat lower than the value expected from the stated accuracies (0.4). This may be caused by condensation of semivolatile gas phase compounds on the large surface of the quartz filters, which is a well-known sampling artifact and constitutes a positive bias of the GC×GC data. For some compounds (such as hopanes and oxygenated PAHs), GC×GC detects less than the TD-PTR-MS. In general, for compounds with mass concentrations below $2\,\mathrm{ng\,m^{-3}}$, the TD-PTR-MS method yielded substantially higher mass concentrations. It should be noted that the 132 compounds measured with the GC×GC technique represent about 10 % of the total OA mass, with another 5–10 % associated with the unresolved complex mixture (UCM) (Chan et al., 2013). There are likely addi-

AMTD
7, 12449–12480, 2014

tional species not quantified with the GC×GC, that are detected as a sum by PTR-MS at the corresponding m/z values.

On the other hand, for alkanes and one amide substantially lower concentrations were detected with the TD-PTR-MS technique (the corresponding points are located at a substantial distance from 1 : 1 line). For alkanes this can be explained by the fact that the main masses at which alkanes are detected (43.055, 57.070, 71.086 Da) were not considered because large contamination from the gas phase did not allow to quantify the condensed fraction. More complicated fragmentation in the PTR-MS can likely explain the lower concentrations found for the amide (N,N-dibutyl-formamide). For all compounds of the class of alkanoic acids (except for decanoic acid), the concentrations were measured to be lower by the TD-PTR-MS, which is likely caused by a positive sampling artifact that is common to quartz filter collection. The latter will be discussed in the following section.

3.2.3 Alkanoic acids

The four alkanoic acids shown in Fig. 4 as black crosses in a red oval are n-dodecanoic, n-tridecanoic, n-tetradecanoic and n-hexadecanoic acids. These 4 compounds are among the most abundant species measured by the GC×GC (3 among the 7 compounds with the highest concentrations, see Fig. 4). To calculate the mass concentrations of the alkanoic acids measured with the in-situ TD-PTR-MS technique, only the intensity of the parent ion signal was considered and multiplied by the calibration factor (1.45) developed for alkanoic acids (see Sect. 3.1). Even after applying this correction factor, the PTR / (GC×GC) ratios for the acids are below unity (Table 2). The semivolatile nature of the acids is a likely reason for this disagreement, due to known positive filter sampling artifacts and, therefore, overestimation of the mass concentrations obtained with the GC×GC technique. This hypothesis is supported by the fact that positive artifacts have been shown to be more severe on filters with short air sampling duration. For example, Timkovsky et al. (2015) demonstrated substantial positive filter

AMTD
7, 12449–12480, 2014

sampling artifacts on filters sampled for 24 h, which were much reduced with sampling durations of 48 and 72 h.

The fraction of the amount of a compound in the particle phase ($F_{p,i}$, amount in the particle phase divided by the total amount in the particle and the gas phase) can be calculated according to the procedure described by, e.g., Yatavelli et al. (2014). Compounds for which $F_{p,i}$ is significantly lower than unity are considered to be semivolatile. $F_{p,i}$ is calculated based on the activity coefficient, vapor pressure, ambient temperature and total OA mass concentration. We used the average activity coefficient calculated for alkanoic acids (1.6) based on Chandramouli et al. (2003). If a component has an activity coefficient above unity within a mixture, the component has a weaker interaction with other molecules in the condensed phase than with itself, and its effective vapor pressure is higher than the pure component vapor pressure. Vapor pressures for do-, tetra- and hexadecanoic acids (Table 2) have been measured by Cappa et al., 2008. Assuming that the logarithm of the vapor pressure of an alkanoic acid has a linear dependency on the number of carbon atoms in the molecule (Goldstein and Galbally, 2007), we calculate the vapor pressure for tridecanoic acid to be 3.2×10^{-6} hPa using known vapor pressures of do-, tetra- and hexadecanoic acids (Table 2). Using an ambient temperature of 25 °C and total OA of 9.4 µg m^{-3} (measured by the AMS), $F_{p,i}$ was found to be substantially lower than unity for 3 out of the 4 acids (do-,tri- and tetradecanoic acids, Table 2). This confirms their semivolatile nature and their potential to cause positive filter sampling artifacts when gas phase molecules condense on the large surface of the quartz filters. This is also consistent with Sihabut et al. (2005) who observed a high contribution from gas phase to particle phase measurements on filters of alkanoic acids containing between 10 and 14 carbon atoms.

Since $F_{p,i}$ for hexadecanoic acid is unity, it is expected to be fully in the particle phase and is not prone to positive filter sampling artifacts (Table 2). This is again consistent with Sihabut et al. (2005), who showed that only a little contribution to particle phase measurements is observed from gas phase with filter sampling of alkanoic acids containing between 15 and 18 carbon atoms. The PTR / (GC×GC) ratio (0.53) for hexade-

AMTD
7, 12449–12480, 2014

canoic acid is within the expected range (0.4–3.2) given by the combined accuracies of TD-PTR-MS and GC×GC. However, further study is needed to exclude the possibility that this low ratio may have resulted from a negative sampling artifact for the in-situ TD-PTR-MS.

We also compared our results to Williams et al. (2010) and found that they experimentally observed on average higher $F_{p,i}$ values for alkanoic acids: 0.92, 1.0 and 1.0 for do-, tri- and hexadecanoic acid, respectively. This might relate to the fact that for measuring gas phase fractions they applied Teflon filters to remove particle phase components, which could, however, also remove a part of the gas phase compounds, causing the obtained $F_{p,i}$ values to be overestimated.

The full two-day time series for the four alkanoic acids obtained with the TD-PTR-MS and the GC×GC method are presented in Fig. 5. The clear diurnal cycle detected by the TD-PTR-MS for all four acids indicates consistency of the measurements. The cycle is also consistent with the diurnal variation of semivolatile compounds observed by the TD-PTR-MS (Holzinger et al., 2013) and the AMS (Hayes et al., 2013) during the same field campaign. The highest correlation coefficient (r, 0.69) between the TD-PTR-MS and GC×GC measurements is observed for hexadecanoic acid among the four acids (Table 2), which is the most abundant and least volatile compound within this compound group. It is mainly present in the particle phase, and thus is subject to relatively low positive filter sampling artifacts (Fig. 5d). Poor correlation is observed for tri- and tetradecanoic acid (Fig. 5b and c, respectively) which is likely caused by the semivolatile nature of the acids and potential measurement artifacts by the GC×GC technique. The latter may be due to the fact that the acids were not derivatized prior to GC×GC analysis. For dodecanoic acid a reasonable qualitative correlation is observed. However, quantitative agreement is poorer than for the other measured acids, which is likely caused by the relatively high volatility of the acid. As shown in Timkovsky et al. (2015), the larger concentrations measured by GC×GC may be caused by condensation of the gas phase fraction of the acids during filter sampling. The poor correlation for tri- and tetradecanoic acid is currently not understood.

AMTD
7, 12449–12480, 2014

4 Conclusions

A comparison of the in-situ TD-PTR-MS and offline quartz filter analysis by the GC×GC/TOF-MS technique, the calibration measurements with the offline TD-PTR-MS technique, and the general comparison of the in-situ TD-PTR-MS and the aerosol mass spectrometer (AMS) technique have been presented. Overall, a reasonable agreement is observed for temporal changes in the bulk organic aerosol (OA) between the AMS and TD-PTR-MS with correlation coefficient of 0.84 (r^2). Reasonable agreement is also observed between temporal changes in the 123 compounds measured from quartz filters by the GC×GC/TOF-MS and the 64 corresponding masses detected by the TD-PTR-MS, with r^2 of 0.67.

The calibration measurements showed that n-alkanoic acids with molecular mass (M_r) below 290 amu are detected at recovery fractions above 60 %. Monocarboxylic acids heavier than 300 amu, and monocarboxylic acids containing double bonds in the mass range $226 < M_r < 290$ amu exhibit recovery fractions below 4 and 38 %, respectively. This is likely caused by the fact that higher temperatures are needed to desorb these compounds from the filters and that thermal decomposition starts taking place before the compounds are fully desorbed. Future measurements of other light unsaturated acids ($M_r < 226$ amu) are needed to test whether their recovery fractions are close to unity, as it is the case for light alkanoic acids ($M_r < 290$ amu). Based on the measured recovery fractions of n-alkanoic acid ($M_r < 290$ amu) measurements, a calibration factor of 1.45 has been established and applied to the in-situ TD-PTR-MS measurements of alkanoic acids ($M_r < 290$ amu).

For the comparison of the in-situ TD-PTR-MS and the offline GC×GC/TOF-MS technique, 123 of 132 compounds measured by the GC× GC/TOF-MS could be matched with ions measured by the PTR-MS. The applied mass matching algorithm took the loss of a water molecule into account, while other fragmentation patterns were not considered. The comparison indicated that the techniques agree reasonably well for single compounds: for most compounds with mass concentrations above 2 ng m^{-3} the

AMTD
7, 12449–12480, 2014

PTR / (GC×GC) ratio was between 0.25 and 2. Compounds detected at levels below 2 ng m^{-3} with the GC×GC/TOF-MS exhibited higher concentrations at the corresponding ions detected by the TD-PTR-MS. This is likely caused by other organic compounds that were detected by the TD-PTR-MS at the corresponding m/z values, but were not specifically identified with the GC×GC/TOF-MS technique (only 132 compounds were identified out of the ∼ 1100 resolved peaks).

All classes of compounds were detected well by the TD-PTR-MS, except for alkanes. The positive filter sampling artifacts, caused by the semivolatile nature of the do-, tri- and tetradecanoic acids, likely resulted in the higher concentrations observed by the GC×GC/TOF-MS and lower correlations between the GC×GC/TOF-MS and TD-PTR-MS measurements.

The Supplement related to this article is available online at doi:10.5194/amtd-7-12449-2014-supplement.

Acknowledgements. The PTR-TOF-MS has been funded by the Netherlands Organization for Scientific Research (NWO) under the ALW-Middelgroot program (Grant 834.08.002). Deployment of the PTR-TOF-MS at CalNex and the analysis using GC×GC/TOF-MS at UC Berkeley were supported by the National Oceanic and Atmospheric Administration (Grant NA10OAR4310104). We would like to acknowledge Patrick Hayes and Jose Jimenez for providing the AMS data. We would like to thank Gabriel Isaacman for preparing the filters with standard mixture. The authors gratefully acknowledge the NOAA Air Resources Laboratory (ARL) for the provision of the HYSPLIT transport and dispersion model and/or READY website (http://www.ready.noaa.gov) used in this publication.

References

Boucher, O., Randall, D., Artaxo, P., Bretherton, C., Feingold, G., Forster, P., Kerminen, V.-M., Kondo, Y., Liao, H., Lohmann, U., Rasch, P., Satheesh, S. K., Sherwood, S., Stevens, B.,

AMTD
7, 12449–12480, 2014

and Zhang, X. Y.: Clouds and aerosols, in: Climate Change 2013: The Physical Science Basis. Contribution of Working Group I to the Fifth Assessment Report of the Intergovernmental Panel on Climate Change, edited by: Stocker, T. F., Qin, D., Plattner, G.-K., Tignor, M., Allen, S. K., Boschung, J., Nauels, A., Xia, Y., Bex, V., and Midgley, P. M., Cambridge University Press, Cambridge, UK, New York, NY, USA, 571–657, 2013.

Cappa, C. D., Lovejoy, E. R., and Ravishankara, A. R.: Evaporation rates and vapor pressures of the even-numbered C_8–C_{18} monocarboxylic acids, J. Phys. Chem. A, 112, 3959–3964, 2008.

Chan, A. W. H., Isaacman, G., Wilson, K. R., Worton, D. R., Ruehl, C. R., Nah, T., Gentner, D. R., Dallmann, T. E., Kirchstetter, T. W., Harley, R. A., Gilman, J. B., Kuster, W. C., de Gouw, J. A., Offenberg, J. H., Kleindienst, T. E., Lin, Y. H., Rubitschun, C. L., Surratt, J. D., Hayes, P. L., Jimenez, J. L., and Goldstein, A. H.: Detailed chemical characterization of unresolved complex mixtures in atmospheric organics: insights into emission sources, atmospheric processing, and secondary organic aerosol formation, J. Geophys. Res.-Atmos., 118, 6783–6796, doi:10.1002/jgrd.50533, 2013.

Chandramouli, B., Jang, M., and Kamens, R. M.: Gas–particle partitioning of semi-volatile organics on organic aerosols using a predictive activity coefficient model: analysis of the effects of parameter choices on model performance, Atmos. Environ., 37, 853–864, 2003.

De Gouw, J. and Jimenez, J. L.: Organic aerosols in the Earth's atmosphere, Environ. Sci. Technol., 43, 7614–7618, doi:10.1021/es9006004, 2009.

DeCarlo, P. F., Kimmel, J. R., Trimborn, A., Northway, M. J., Jayne, J. T., Aiken, A. C., Gonin, M., Fuhrer, K., Horvath, T., Docherty, K. S., Worsnop, D. R., and Jimenez, J. L.: Field-deployable, high-resolution, time-of-flight aerosol mass spectrometer, Anal. Chem., 78, 8281–8289, 2006.

Draxler, R. R. and Rolph, G. D.: HYSPLIT (Hybrid single-particle lagrangian integrated trajectory) Model access via NOAA ARL READY Website (http://www.arl.noaa.gov/HYSPLI~T.php), NOAA Air Resources Laboratory, College Park, MD, 2013.

Goldstein, A. H. and Galbally, I. E.: Known and unexplored organic constituents in the Earth's atmosphere, Environ. Sci. Technol., 41, 1514–1521, 2007.

Hamilton, J. F., Webb, P. J., Lewis, A. C., Hopkins, J. R., Smith, S., and Davy, P.: Partially oxidised organic components in urban aerosol using GCXGC-TOF/MS, Atmos. Chem. Phys., 4, 1279–1290, doi:10.5194/acp-4-1279-2004, 2004.

AMTD
7, 12449–12480, 2014

Hayes, P. L., Ortega, A. M., Cubison, M. J., Froyd, K. D., Zhao, Y., Cliff, S. S., Hu, W. W., Toohey, D. W., Flynn, J. H., Lefer, B. L., Grossberg, N., Alvarez, S., Rappenglück, B., Taylor, W., Allan, J. D., Holloway, J. S., Gilman, J. B., Kuster, W. C., de Gouw, J. A., Massoli, P., Zhang, X., Liu, J., Weber, R. J., Corrigan, A. L., Russell, L. M., Isaacman, G., Worton, D. R., Kreisberg, N. M., Goldstein, A. H., Thalman, R., Waxman, E. M., Volkamer, R., Y. H.Lin, Surratt, J. D., Kleindienst, T. E., Offenberg, J. H., Dusanter, S., Griffith, S., Stevens, P. S., Brioude, J., Angevine, W. M., and Jimenez, J. L.: Organic aerosol composition and sources in Pasadena, California, during the 2010 CalNex campaign, J. Geophys. Res.-Atmos., 118, 9233–9257, doi:10.1002/jgrd.50530, 2013.

Holzinger, R., Williams, J., Herrmann, F., Lelieveld, J., Donahue, N. M., and Röckmann, T.: Aerosol analysis using a Thermal-Desorption Proton-Transfer-Reaction Mass Spectrometer (TD-PTR-MS): a new approach to study processing of organic aerosols, Atmos. Chem. Phys., 10, 2257–2267, doi:10.5194/acp-10-2257-2010, 2010a.

Holzinger, R., Kasper-Giebl, A., Staudinger, M., Schauer, G., and Röckmann, T.: Analysis of the chemical composition of organic aerosol at the Mt. Sonnblick observatory using a novel high mass resolution thermal-desorption proton-transfer-reaction mass-spectrometer (hr-TD-PTR-MS), Atmos. Chem. Phys., 10, 10111–10128, doi:10.5194/acp-10-10111-2010, 2010b.

Holzinger, R., Goldstein, A. H., Hayes, P. L., Jimenez, J. L., and Timkovsky, J.: Chemical evolution of organic aerosol in Los Angeles during the CalNex 2010 study, Atmos. Chem. Phys., 13, 10125–10141, doi:10.5194/acp-13-10125-2013, 2013.

Jayne, J. T., Leard, D. C., Zhang, X. F., Davidovits, P., Smith, K. A., Kolb, C. E., and Worsnop, D. R.: Development of an aerosol mass spectrometer for size and composition analysis of submicron particles, Aerosol Sci. Tech., 33, 49–70, 2000.

Kallio, M., Jussila, M., Rissanen, T., Anttila, P., Hartonen, K., Reissell, A., Vreuls, R., Adahchour, M., and Hyötyläinen, T.: Comprehensive two-dimensional gas chromatography coupled to time-of-flight mass spectrometry in the identification of organic compounds in atmospheric aerosols from coniferous forest, J. Chromatogr. A, 1125, 234–43, doi:10.1016/j.chroma.2006.05.050, 2006.

Kanakidou, M., Seinfeld, J. H., Pandis, S. N., Barnes, I., Dentener, F. J., Facchini, M. C., Van Dingenen, R., Ervens, B., Nenes, A., Nielsen, C. J., Swietlicki, E., Putaud, J. P., Balkanski, Y., Fuzzi, S., Horth, J., Moortgat, G. K., Winterhalter, R., Myhre, C. E. L., Tsigaridis, K.,

AMTD
7, 12449–12480, 2014

Vignati, E., Stephanou, E. G., and Wilson, J.: Organic aerosol and global climate modelling: a review, Atmos. Chem. Phys., 5, 1053–1123, doi:10.5194/acp-5-1053-2005, 2005.
Kawamura, K. and Sakaguchi, F.: Molecular distributions of water soluble dicarboxylic acids in marine aerosols over the Pacific Ocean including tropics, J. Geophys. Res., 104, 3501–3509, 1999.
Legrand, M. and De Angelis, M.: Light carboxylic acids in Greenland ice? A record of past forest fires and vegetation emissions from the boreal zone, J. Geophys. Res., 101, 4129–4145, 1996.
Pope, C. A. and Dockery, D. W.: Health effects of fine particulate air pollution? Lines that connect, J. Air Waste Manage., 56, 709–742, 2006.
Rolph, G. D.: Real-time environmental applications and Display system (READY) website, available at: http://www.ready.noaa.gov (last access: 21 July 2014), NOAA Air Resources Laboratory, College Park, MD, 2013.
Sihabut, T., Ray, J., Northcross, A., and McDow, S. R.: Sampling artifact estimates for alkanes, hopanes, and aliphatic carboxylic acids, Atmos. Environ., 39, 6945–6956, doi:10.1016/j.atmosenv.2005.02.053, 2005.
Timkovsky, J., Dusek, U., Henzing, J. S., Kuipers, T. L., Röckmann, T., and Holzinger, R. Offline thermal-desorption proton-transfer-reaction mass spectrometry to study composition of organic aerosol, J. Aerosol Sci., 79, 1–14, doi:10.1016/j.jaerosci.2014.08.010, 2015.
Ulbrich, I. M., Canagaratna, M. R., Zhang, Q., Worsnop, D. R., and Jimenez, J. L.: Interpretation of organic components from Positive Matrix Factorization of aerosol mass spectrometric data, Atmos. Chem. Phys., 9, 2891–2918, doi:10.5194/acp-9-2891-2009, 2009.
Veres, P. R., Roberts, J. M., Cochran, A. K., Gilman, J. B., Kuster, W. C., Holloway, J. S., Graus, M., Flynn, J., Lefer, B., Warneke, C., and de Gouw, J.: Evidence of rapid production of organic acids in an urban air mass, Geophys. Res. Lett., 38, L17807, doi:10.1029/2011GL048420, 2011.
Vogel, A. L., Äijälä, M., Brüggemann, M., Ehn, M., Junninen, H., Petäjä, T., Worsnop, D. R., Kulmala, M., Williams, J., and Hoffmann, T.: Online atmospheric pressure chemical ionization ion trap mass spectrometry (APCI-IT-MS^n) for measuring organic acids in concentrated bulk aerosol – a laboratory and field study, Atmos. Meas. Tech., 6, 431–443, doi:10.5194/amt-6-431-2013, 2013.

AMTD
7, 12449–12480, 2014

Weber, R. J., Orsini, D., Daun, Y., Lee, Y.-N., Klotz, P. J., and Brechtel, F.: A particle-into-liquid collector for rapid measurement of aerosol bulk chemical composition, Aerosol Sci. Tech., 35, 718–727, doi:10.1080/02786820152546761, 2001.

Williams, B. J., Goldstein, A. H., Kreisberg, N. M., and Hering, S. V.: In situ measurements of gas/particle-phase transitions for atmospheric semivolatile organic compounds, P. Natl. Acad. Sci. USA, 107, 6676–81, doi:10.1073/pnas.0911858107, 2010.

Williams, B. J., Jayne, J. T., Lambe, A. T., Hohaus, T., Kimmel, J. R., Sueper, D., Brooks, W., Williams, L. R., Trimborn, A. M., Martinez, R. E., Hayes, P. L., Jimenez, J. L., Kreisberg, N. M., Hering, S. V., Worton, D. R., Goldstein, A. H., and Worsnop, D. R.: The First Combined Thermal Desorption Aerosol Gas Chromatograph – Aerosol Mass Spectrometer (TAG-AMS), Aerosol Sci. Tech., 48, 358–370, doi:10.1080/02786826.2013.875114, 2014.

Yatavelli, R. L. N., Stark, H., Thompson, S. L., Kimmel, J. R., Cubison, M. J., Day, D. A., Campuzano-Jost, P., Palm, B. B., Hodzic, A., Thornton, J. A., Jayne, J. T., Worsnop, D. R., and Jimenez, J. L.: Semicontinuous measurements of gas–particle partitioning of organic acids in a ponderosa pine forest using a MOVI-HRToF-CIMS, Atmos. Chem. Phys., 14, 1527–1546, doi:10.5194/acp-14-1527-2014, 2014.

Yu, J. Z., Xu, J., and Yang, H.: Charring characteristics of atmospheric organic particulate matter in thermal analysis, Environ. Sci. Technol., 36, 754–761, 2002.

Zhao, J. and Zhang, R. Y.: Proton transfer reaction rate constants between hydronium ion (H_3O^+) and volatile organic compounds, Atmos. Environ., 38, 2177–2185, 2004.

Zhao, Y., Kreisberg, N. M., Worton, D. R., Isaacman, G., Gentner, D. R., Chan, A. W. H., Weber, R. J., Liu, S., Day, D. A., Russell, L. M., Hering, S. V., and Goldstein, A. H.: Sources of organic aerosol investigated using organic compounds as tracers measured during CalNex in Bakersfield, J. Geophys. Res., 118, 11388–11398, doi:10.1002/jgrd.50825, 2013.

AMTD
7, 12449–12480, 2014

Table 1. Molecular formula, masses and fraction recovered of 24 protonated monocarboxylic acids measured as standards on quartz filters individually (in italic) and in the multicomponent mixture. Acids indicated in bold are not detected with the offline TD-PTR-MS technique.

Compound	Molecular formula $\cdot H^+$	Molecular weight	Fraction
Decanoic acid	$C_{10}H_{21}O_2^+$	173.154	0.59
Lauric acid	$C_{12}H_{25}O_2^+$	201.185	0.60
cis-9-Tetradecenoic acid (Myristoleic acid)	$C_{14}H_{27}O_2^+$	227.201	0.38
Myristic acid	$C_{14}H_{29}O_2^+$	229.217	0.80
Pentadecanoic acid	$C_{15}H_{31}O_2^+$	243.232	0.87
cis-9-Hexadecenoic acid (Palmitoleic acid)	$C_{16}H_{31}O_2^+$	255.232	0.23
Palmitic acid	$C_{16}H_{33}O_2^+$	257.248	0.60
cis-10-Heptadecenoic acid	$C_{17}H_{33}O_2^+$	269.248	0.10
cis, cis-9,12-Octadecadienoic acid (Linoleic acid)	$C_{18}H_{33}O_2^+$	281.248	0.03
cis-9-Octadecenoic acid (Oleic acid; Elainic acid)	$C_{18}H_{35}O_2^+$	283.264	0.06
Stearic acid	$C_{18}H_{37}O_2^+$	285.279	0.66
cis-5,8,11,14,17-Eicosapentaenoic acid (Timnodonic acid)	$C_{20}H_{31}O_2^+$	303.232	0.04
cis-11-Eicosenoic acid (Gondoic acid)	$C_{20}H_{39}O_2^+$	311.295	–
cis-13-Docosenoic acid (Erucic acid)	$C_{22}H_{43}O_2^+$	339.326	–
Docosanoic acid (Behinic acid)	$C_{22}H_{45}O_2^+$	341.342	–
Tricosanoic acid	$C_{23}H_{47}O_2^+$	355.358	0.02
cis-15-Tetracosenoic acid (Nervonic acid)	$C_{24}H_{47}O_2^+$	367.358	0.01
Tetracosanoic acid (Lignoceric acid)	$C_{24}H_{49}O_2^+$	369.373	0.02
Pentacosanoic acid	$C_{25}H_{51}O_2^+$	383.389	0.0004
Hexacosanoic acid (Cerotic acid; Cerotinic acid)	$C_{26}H_{53}O_2^+$	397.405	0.0020
Heptacosanoic acid	$C_{27}H_{55}O_2^+$	411.420	0.02
Octacosanoic acid (Montanic acid)	$C_{28}H_{57}O_2^+$	425.436	–
Nonacosanoic acid	$C_{29}H_{59}O_2^+$	439.452	0.0019
Triacontanoic acid (Melissic acid)	$C_{30}H_{61}O_2^+$	453.467	–

AMTD
7, 12449–12480, 2014

Table 2. Calculated partitioning coefficients $F_{p,i}$, observed PTR / (GC×GC) ratios averaged over the considered period, vapor pressures of dodecanoic, tridecanoic, tetradecanoic and hexadecanoic acids, and correlation coefficients (r) of the TD-PTR-MS and the GC×GC measurements of the acids.

Compound	$F_{p,i}$	PTR / (GC×GC) ratio	vapor pressure, hPa	r, 2GC vs. PTR
Dodecanoic acid	0.03	0.25	2.3E-05	0.65
Tridecanoic acid	0.17	0.45	3.2E-06	−0.68
Tetradecanoic acid	0.48	0.31	7.0E-07	0.46
Hexadecanoic acid	1.00	0.53	1.3E-09	0.69

AMTD
7, 12449–12480, 2014

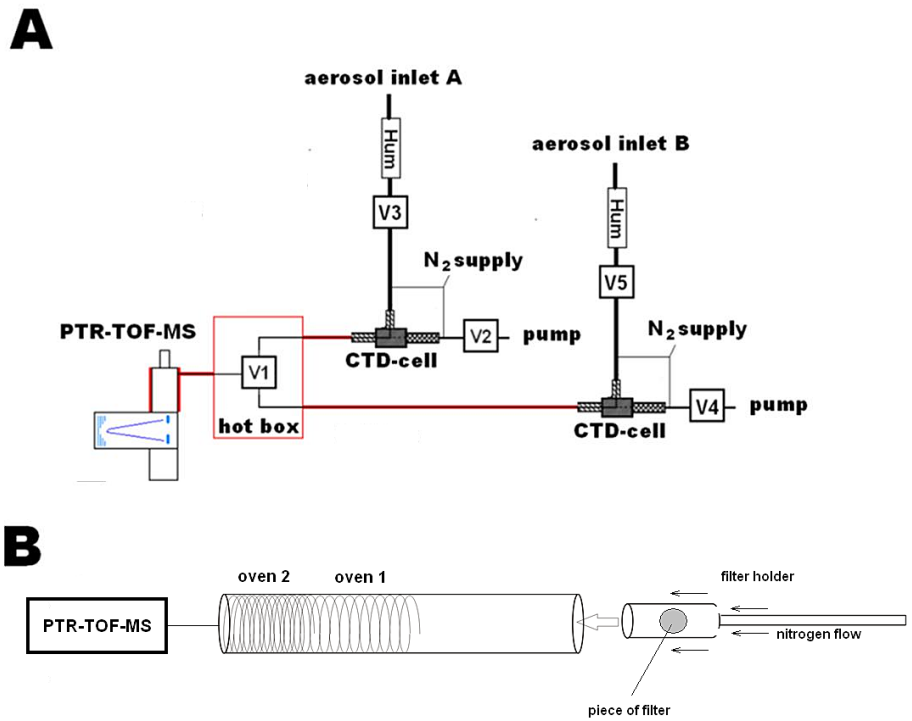

Figure 1. The in-situ **(a)** and offline **(b)** TD-PTR-MS setups. The following valves are present on scheme **(a)**: V1 – allows switching between two aerosol inlets, V2–V5 – allow switching between sampling and measuring modes for inlet A and B. (The figure and the caption are taken from Timkovsky et al., 2015)

AMTD
7, 12449–12480, 2014

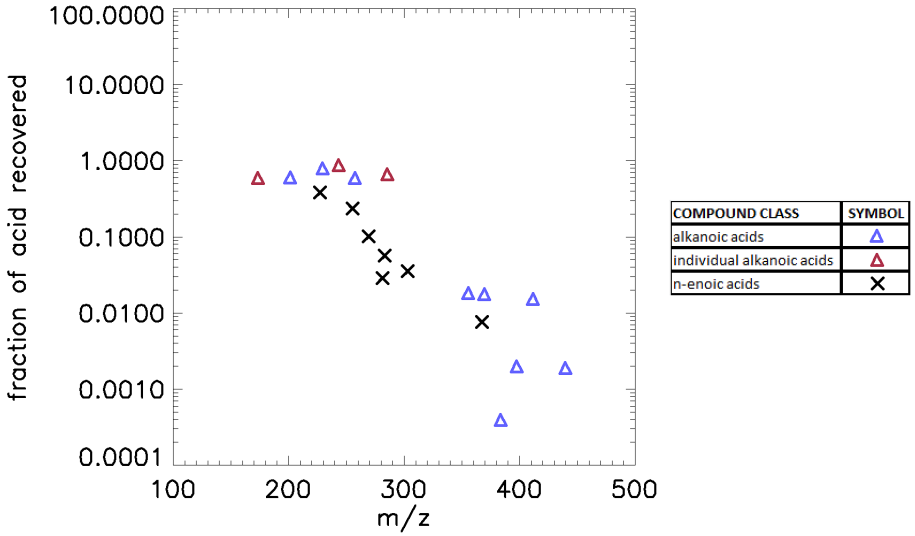

Figure 2. The ratio of the amount of a substance on the filters measured with the offline TD-PTR-MS technique to the known amount of the substance put on the filters (fraction of acid recovered).

AMTD
7, 12449–12480, 2014

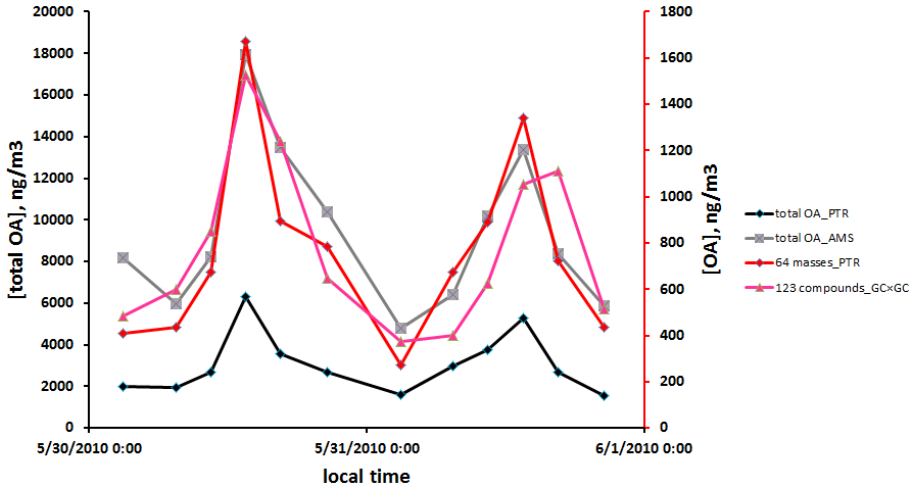

Figure 3. The two day cycle of total OA mass concentration (in black, total OA_PTR) and OA mass concentration of 64 masses (in red) measured with the in-situ TD-PTR-MS technique, and total OA mass concentration (in grey, total OA_AMS) measured by the AMS and OA mass concentration of 123 compounds (in pink) measured with the GC×GC technique. Left *y* axis (in black) corresponds to total OA_PTR and total OA_AMS, and right *y* axis (in red) corresponds to 64 masses_PTR and 123 compounds_GC×GC.

AMTD
7, 12449–12480, 2014

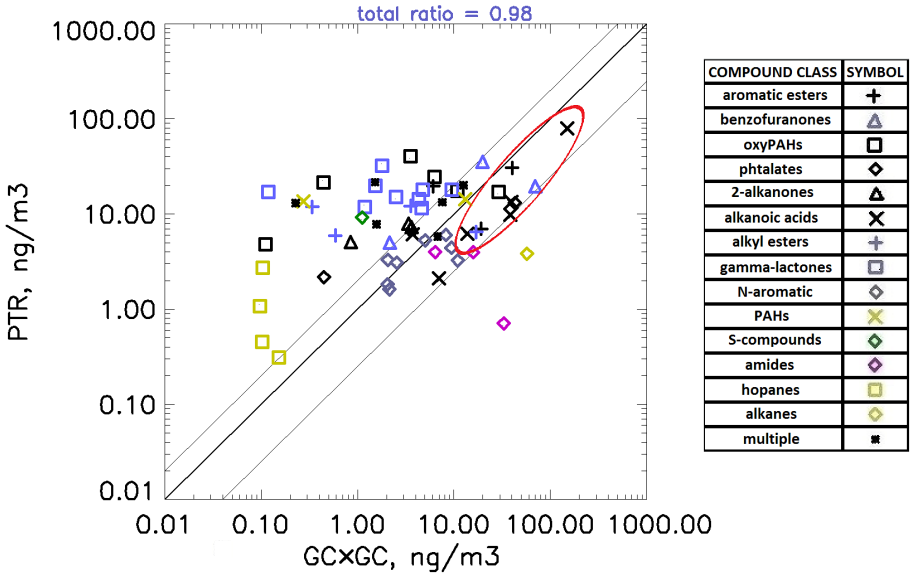

Figure 4. Comparison of aerosol mass concentrations measured with the in-situ TD-PTR-MS and GC×GC technique. The legend shows classes of compounds depicted, which are described in detail in the text. The total PTR / (GC×GC) ratio is 0.98. The red oval highlights (among other species) four alkanoic acids which are discussed in Sect. 3.2.3. The thin diagonal lines indicate the upper and lower boundaries of the reasonable PTR / (GC×GC) ratio (0.25 and 2).

AMTD
7, 12449–12480, 2014

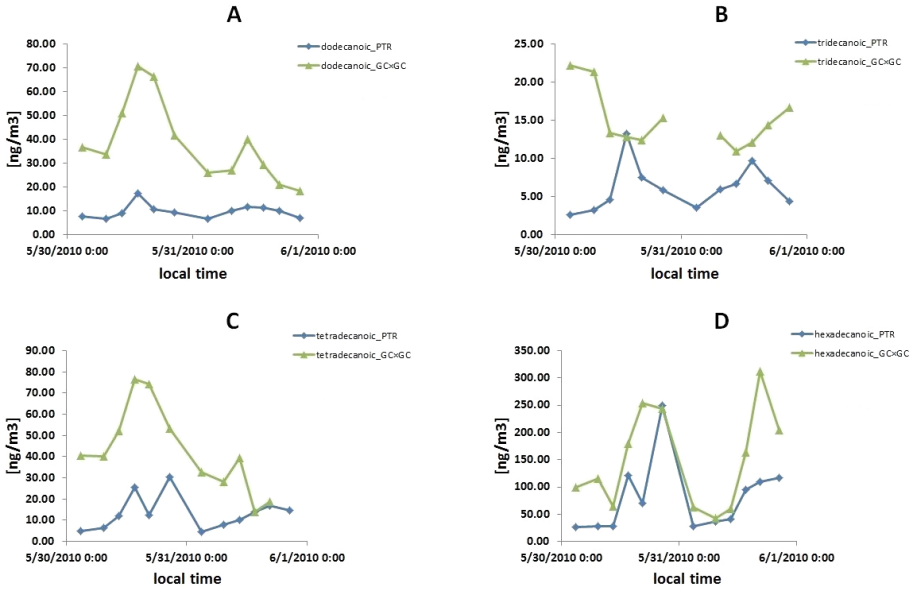

Figure 5. Time profiles for mass concentrations measured with the TD-PTR-MS and the GC×GC techniques for four alkanoic acids: dodecanoic **(a)**, tridecanoic **(b)**, tetradecanoic **(c)** and hexadecanoic **(d)**.

AMTD
7, 12449–12480, 2014